Monatshefte für Chemie - Chemical Monthly (2020) 151:353–367
https://doi.org/10.1007/s00706-020-02561-1

ORIGINAL PAPER

Synthesis and biological evaluation of new mono naphthalimide platinum(IV) derivatives as antitumor agents with dual DNA damage mechanism

Zuojie Li[1] · Yan Chen[1] · Zhifang Liu[1] · Qingpeng Wang[1] · Yanna Zhao[1] · Jinjian Wei[2] · Min Liu[1] · Zhengping Wang[1] · Dacheng Li[1,3] · Jun Han[1]

Received: 20 December 2019 / Accepted: 10 February 2020 / Published online: 26 February 2020

Abstract

Naphthalimide has emerged as an interesting DNA intercalator and possessed attracting antitumor properties. In this context, naphthalimide group was linked to platinum(IV) core to construct a series of new mono naphthalimide platinum(IV) derivatives. The title compounds exert effective antitumor activities to the tested tumor cells lines in vitro, especially the one with propionyl chain displays comparable or even better bioactivities than platinum(II) reference drugs cisplatin and oxaliplatin. Moreover, the mono naphthalimide platinum(IV) derivative displays comparable tumor growth inhibitory competence against CT26 xenograft tumors in BALB/c mice in vivo without severe toxic effects in contrast to oxaliplatin. A dual DNA damage mechanism was proven for the title complex. Both naphthalimide ligand and the liberated platinum(II) moiety could generate DNA lesions to tumor cells synergistically and active the apoptotic pathway by up-regulating the expression of caspase 9 and caspase 3. Meanwhile, the conversion of platinum(II) drug into tetravalent form by incorporating naphthalimide moiety increases the uptake of platinum in whole cells and DNA remarkably. All these facts might be the factors for the title platinum(IV) complexes to overcome platinum(II) drug resistance. Additionally, the mono naphthalimide platinum(IV) complex could interact with human serum albumin by hydrogen bond and van der Waals force which would further influence their storage, transport and bioactivities.

Graphic abstract

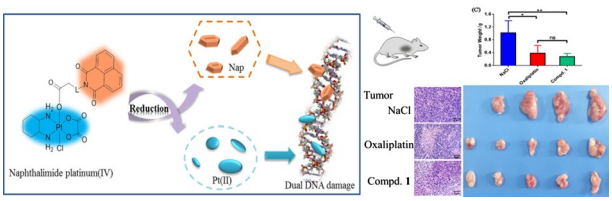

Keywords Platinum · Antitumor · Naphthalimide · DNA damage · Prodrugs

Electronic supplementary material The online version of this article (https://doi.org/10.1007/s00706-020-02561-1) contains supplementary material, which is available to authorized users.

✉ Qingpeng Wang
lywqp@126.com

✉ Min Liu
panpanliumin@163.com

✉ Dacheng Li
lidacheng62@163.com

[1] Institute of Biopharmaceutical Research, Liaocheng University, Liaocheng 252059, People's Republic of China

[2] College of Chemistry, Chemical Engineering and Materials Science, Shandong Normal University, Jinan 250014, People's Republic of China

[3] Shandong Provincial Key Laboratory of Chemical Energy Storage and Novel Cell Technology, Liaocheng University, Liaocheng 252059, People's Republic of China

Introduction

Cancer is ranked as a leading cause of death for its high incidence and mortality worldwide. Chemotherapies play extremely significant roles in the treatment of malignancies [1, 2]. The discovery and market of platinum(II) drugs led to the development of metal chemotherapeutics to a new era [3, 4]. In spite of the great achievements of platinum(II) drugs, their applications in clinic were badly restrained by severe side effects and easily acquired drug resistance rising from premature equation and high chemical reactivity [5, 6]. Thereby, it is urgent to develop new prominent platinum candidates with high stability and low toxicity to defeat inherent drawbacks of platinum(II) compounds.

Platinum(IV) complexes as versatile prodrugs of platinum(II) drugs are of great potential to be developed as the next generation of platinum drugs. So far, several outstanding ones including satraplatin (JM216), ormaplatin, iproplatin (JM9), and LA-12 have stepped into clinical trials (Fig. 1) and displayed many unique advantages in contrast to platinum(II) drugs such as better stable properties, longer half-life in blood, lower toxicity [7–11]. Additionally, the easy modification of the axial ligands in platinum(IV) afforded a convenient way to construct new complexes with multifunctional active mechanism by incorporating various functional groups and further transferring desired properties to platinum(IV) system [12–15]. The exploration of novel platinum(IV) antitumor complexes especially the ones with unique acting mechanisms has become an attractive strategy to develop new platinum drugs.

Naphthalimide derivatives as promising DNA intercalators were widely investigated as antineoplastic drugs, and would potentially induce apoptosis of tumor cells by causing serious DNA damage [16–18]. It was found that conjunct of naphthalimide to platinum system led significant positive effects on the improvement of antitumor activities. Naphthalimide conspicuously enhance the DNA damage of platinum drugs to tumor cells by causing a synergetic DNA lesion, which would reduce the off-target effects of platinum complex and further favor for overcoming drug resistance. So far, many naphthalimide platinum hybrids such as complexes **I**–**IX** with prominent activities have been developed (Fig. 1) [19–24]. Especially, naphthalimide serving as a "carrier" of drugs incorporated into platinum(IV) complexes **VII** and **VIII** remarkably increased their DNA targeting and bioactivities. Then, in our previous work, complex **IX** with double naphthalimide axial ligands were prepared and exhibited antitumor activities via a dual DNA damage mechanism. Nevertheless, some shortcomings of these serial complexes especially the poor solubility in water seriously influenced their bioactivities. Furthermore, platinum(IV) complex **X** with mono naphthalimide axial ligand displayed more effective antitumor activities than **IX**. Thereby, it is of great interest for us to develop more effective naphthalimide platinum(IV) complexes as antitumor agents based on such scaffold.

Inspired by these situations and in continuation of our ongoing interests in the development of novel antitumor agents [25–28], we would like to design a series of mono naphthalimide modified platinum(IV) compounds to evaluate their antitumor properties. Furthermore, a mono aminonaphthalimide platinum(IV) complex **X** has been reported in our previous work and possessed potent antitumor activities and interesting mechanism [29]. To further develop effective antitumor agents based on such scaffold, a series of related compounds **1**–**4** were designed and prepared to learn their structure activities relationships (Fig. 2). The naphthalimide moiety was introduced to platinum(IV) system purposed to prepare target compounds with dual DNA damage mechanism. The mono naphthalimide platinum(IV) compounds **1**–**4** with smaller molecule than complexes **IX** would improve the solubility of title compounds and further influencing their bioactivities. As is well known, oxaliplatin has been successfully developed as the third generation of platinum drug to overcome resistance against cisplatin and carboplatin and internationally marketed for the treatment of human neoplasms. Aiming at gaining prominent platinum(IV) compounds with drug resistance overcoming properties, oxaliplatin was employed as the core of the platinum(IV) drugs. Furthermore, to detect the influence of linkage on the activities, complexes **1**–**3** with different linkers were designed. Moreover, it has been proven that the incorporation of nitrogen-containing groups onto naphthalimide fragment showed many impacts on the bioactivities [23, 24, 30]. Thus, compound **4** bearing nitro moiety was prepared to compare with complexes **2** and **X**. The structures of all the title compounds were characterized and the antitumor activities were evaluated. Their likely action mechanism was also detected.

Results and discussion

Chemistry

Compounds **1**–**4** were synthesized by the condensation of naphthalimide acids **A1**–**A4** with oxoplatin **O1** (Scheme S1). The acids **A1**–**A4** were synthesized by the literature procedures with 1,8-naphthalic anhydride and amino acids as starting materials [23, 24]. The oxidation of oxaliplatin in the presence of *N*-chlorosuccinimide (NCS) produced oxoplatin **O1**. Subsequently, the combination of naphthalimide acids

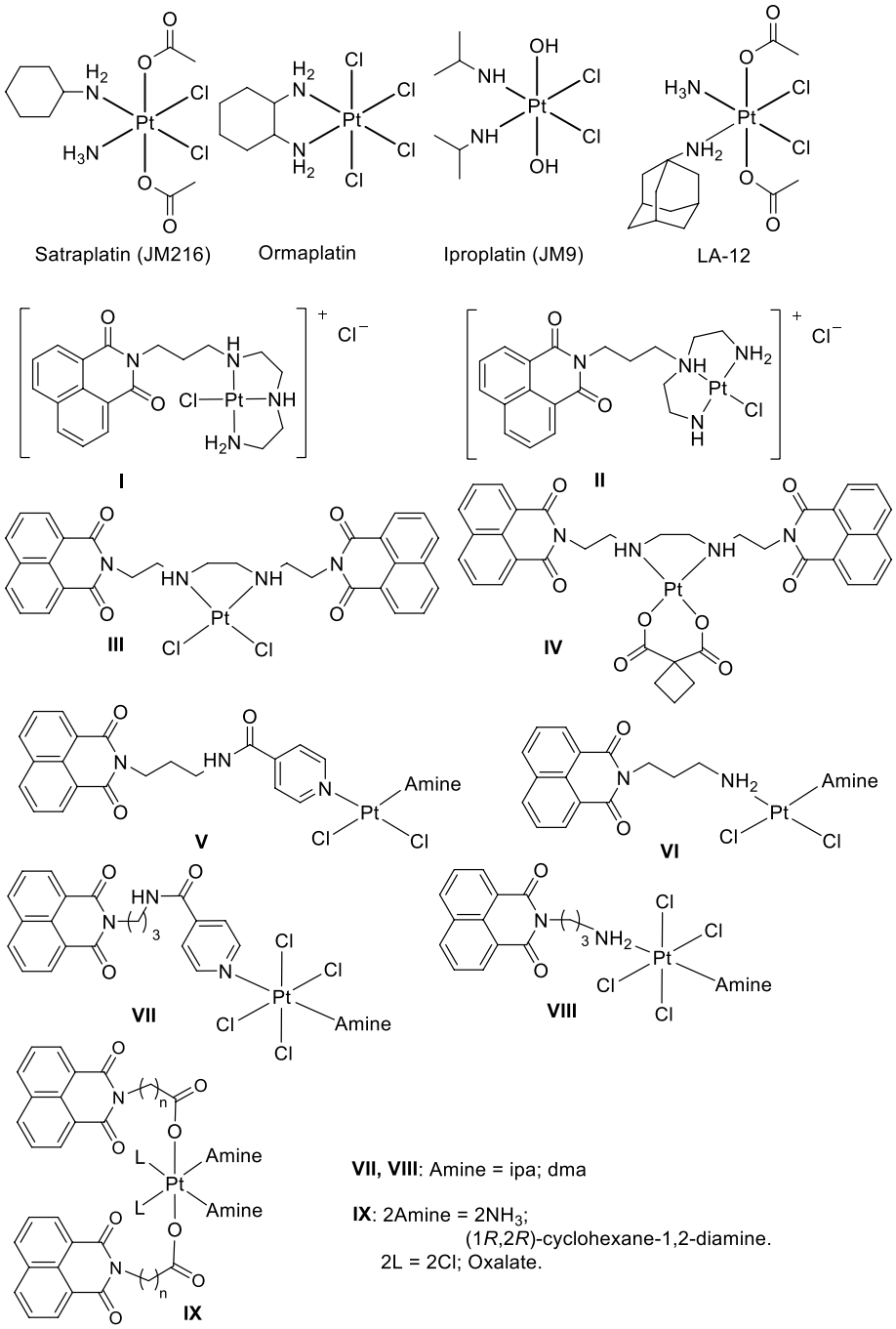

Fig. 1 Chemical structures of platinum(IV) drugs entered clinic trials and naphthalimide platinum(IV) compounds

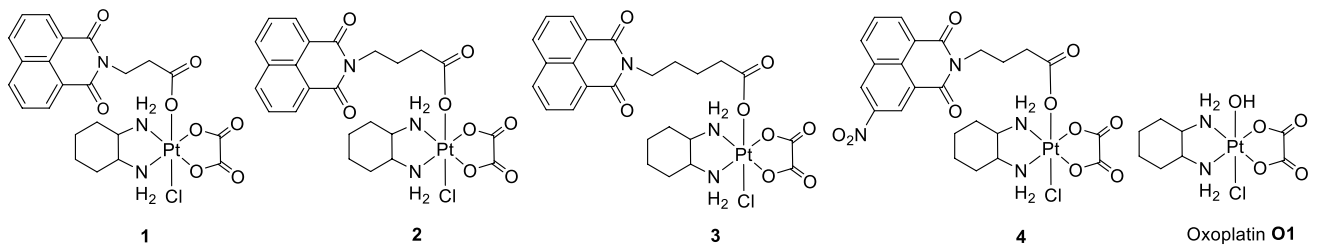

Fig. 2 Structures of mono naphthalimide platinum(IV) compounds **1**–**4** and oxoplatin **O1**

and oxoplatin **O1** in dry *N*,*N*-dimethylformamide (DMF) in the presence of *N*,*N*,*N*′,*N*′-tetramethyl-*O*-(benzotriazol-1-yl)-uronium tetrafluoroborate (TBTU) and triethylamine (TEA) afforded compounds **1**–**4** in yields of 25–27%. These compounds were characterized by IR, ^{1}H NMR, ^{13}C NMR and HRMS. The melting points were also tested.

Antitumor activities in vitro

To explore the potential of the title compounds as antitumor agents, their antiproliferative abilities were monitored toward five cancer cell lines including human ovarian cancer (SKOV-3), human cervical cancer (HeLa), human lung cancer (A549), cisplatin-resistant cell A549R, and murine colon cancer (CT26). Moreover, one normal human cell line embryonic kidney cell (293T) was also tested to evaluate their toxic properties.

The cytotoxicity profiles in Table 1 indicate that mono naphthalimide platinum(IV) compounds **1**–**4** exert wide spectrum antitumor activities with IC_{50} values below 26.5 μM to the five tested cancer cell lines. They are more competent than the corresponding dual naphthalimide substituted platinum(IV) compounds **IX** [23, 24], which are probably ascribed to the enhanced solubility of the title compounds (Table S3). Then, in comparison with complexes **1**–**4**, the naphthalimide acid **A1** and oxoplatin **O1** display weak antitumor bioactivities, and the mixture of **A1** with **O1** (**A1&O1**) leads no enhancements of the activities. It could be concluded that the conjunction of naphthalimide with platinum(IV) emerges as a promising strategy to enhance antitumor competence.

Moreover, the designed compounds are of much potential in overcoming drug resistance of cisplatin. Especially, compounds **1** and **2** could almost fully defeat the resistance of A549R by reducing the resistant factor (RF) from 1.7 for cisplatin to 0.7. However, as for the normal human cell line, the title complexes also display effective inhibition on the 293T cells. It seems that this series of compounds possess no improved tumor-targeting properties in comparison with platinum(II) drugs.

Structurally, the variation of the linkage between platinum(IV) and naphthalimide moieties leads many impacts on the bioactivities, meanwhile the incorporation of nitro moiety onto naphthalimide also influences their antitumor competence to some extent. Short linker is more suitable for the antitumor activities of these compounds, and compound **1** with propionyl chain exhibits the most prominent activities to all tested tumor cells ($IC_{50} \leq 10.7$ μM) which are more effective than cisplatin and oxaliplatin. Then the activities of compounds **2** and **3** decrease to some extent in contrast to complex **1** when the chains prolong to butyryl and valeryl moieties. Furthermore, the introduction of nitro group into compound **2** to form compound **4** displays some influence on the antitumor efficacy. It decreases the activities toward SKOV-3 and A549R in contrast to compound **2** and increases the efficacy against A549 and CT26 to some extent. Moreover, the nitronaphthalimide platinum(IV) complexes **4** displays relatively lower antitumor activities in comparison with aminonaphthalimide derived compound **X** [29], which demonstrates that hydrophilic amino group seems more favorable for enhancing activities for mono naphthalimide platinum(IV) complex. Accordingly, the results above enable these compounds to be of much potential for further investigations as new antitumor agents, and compound **1** with the most prominent activities was screed out for further evaluation as an antitumor candidate.

Antitumor activities in vivo

To further determine the potential of the title mono naphthalimide platinum(IV) derivatives as antitumor agents, the bioactive properties in vivo of prominent compound **1** were evaluated with oxaliplatin as positive reference drug. It was proven that the immune system was important for

Table 1 Cytotoxicity profiles of mono naphthalimide platinum(IV) complexes toward four human carcinoma cell lines, one murine carcinoma cell line, and one normal human cell line expressed as IC_{50} (μM)

Compounds	SKOV-3	Hela	A549	A549R	RF[a]	CT26	293T
1	2.8 ± 0.4	2.0 ± 0.2	10.7 ± 0.7	7.3 ± 1.5	0.7	6.2 ± 0.9	14.0 ± 1.6
2	3.4 ± 0.3	2.5 ± 0.6	17.2 ± 1.9	12.8 ± 2.0	0.7	6.5 ± 0.7	5.1 ± 0.5
3	3.6 ± 0.6	2.9 ± 0.3	12.5 ± 1.5	15.9 ± 1.7	1.3	11.1 ± 1.6	9.0 ± 1.3
4	6.4 ± 1.1	2.9 ± 0.5	9.51 ± 1.2	26.5 ± 4.2	2.8	3.2 ± 0.4	9.8 ± 1.0
O1	11.3 ± 0.9	6.7 ± 0.7	28.0 ± 2.5	43.8 ± 8.3	1.6	12.6 ± 2.7	11.3 ± 0.7
A1	≥ 100	≥ 100	73.2 ± 16.4	≥ 100	NC[b]	≥ 100	88.3 ± 10.7
O1&A1[c]	15.6 ± 2.2	7.5 ± 0.8	43.7 ± 5.3	46.6 ± 6.0	1.1	18.4 ± 4.8	9.3 ± 0.6
Cisplatin	2.4 ± 0.2	2.4 ± 0.5	13.5 ± 2.1	22.6 ± 3.2	1.7	5.3 ± 1.9	12.2 ± 0.5
Oxaliplatin	5.3 ± 0.4	7.4 ± 1.0	26.8 ± 3.8	22.2 ± 1.8	0.8	3.9 ± 0.8	2.7 ± 0.4

[a] *RF* resistant factor. $RF(A549) = IC_{50}(A549R)/IC_{50}(A549)$

[b] *NC* not calculated

[c] **O1&A1**: 1 equivalents of acid **A1** mixed with 1 equivalent of oxoplatin **O1**

the anticancer activity of oxaliplatin as well as oxaliplatin derivatives, and the immunocompetent BALB/c mice were good models for oxaliplatin derived platinum(IV) complexes [31, 32]. Thereby, compound **1** was evaluated for antitumor activities in BALB/c mice bearing CT26 xenograft tumors. The results in Fig. 3 manifest that compound **1** could effectively inhibit the growth of tumor in comparison with the untreated group (NaCl), which is comparable to oxaliplatin (Fig. 3a, c, f). Then compound **1** exerts slight impact on the bodyweight of the mice during the treatment which is relatively better than oxaliplatin, and these results prove that compound **1** induces no severe toxic influence on the mice during 12 days treatment at such dosage (Fig. 3b). Then on day 19, 1 day after the last treatment with platinum drugs, the mice were killed and organs were collected. The hematoxylin and eosin (H&E) staining of slices from heart, lung, liver, spleen, and kidney (Fig. 3d) indicates that normal tissues from mice treated with compound **1** have quite similar structures and histological features with the tissues of the untreated mice, and compound **1** exhibits hardly toxic effects

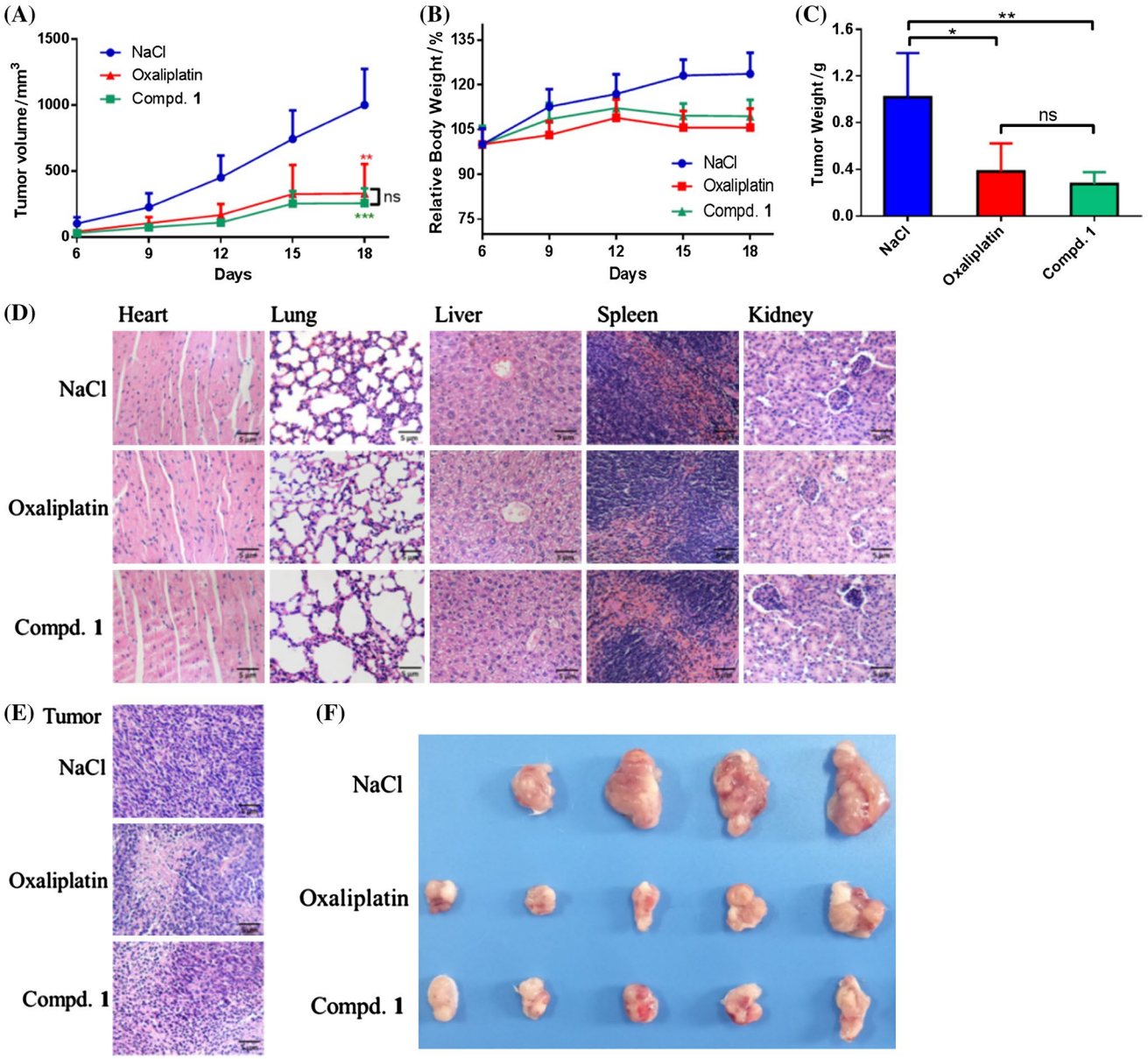

Fig. 3 In vivo antitumor activities of compound **1** and oxaliplatin to CT26 xenograft tumors in BALB/c mice. **a** Tumor growth as a function of time. **b** The bodyweight of the mice during the treatment. **c** The tumor weight in each group at the end of the experiment. **d** The H&E staining of slices from heart, lung, liver, spleen, and kidney. **e** The H&E staining of slices from tumor. **f** The images of the tumors at the end of the experiment. Results are representative of at least three independent experiments and shown as the mean ± SD. $*p<0.05$, $**p<0.01$, $***p<0.001$, *ns* no significant difference compared with control group

on normal tissues in contrast to oxaliplatin. As for the tumor tissues (Fig. 3e), the platinum(IV) complex **1** induces obvious histological change in contrast to the control group, and the average tumor cell numbers in each microscopic field reduces significantly, which are similar to that of oxaliplatin. Accordingly, the naphthalimide platinum(IV) complex could significantly inhibit the growth of CT-26 tumor in vivo and displays no remarkable toxic effects which are comparable or even better than oxaliplatin. Thereby, platinum(IV) complex **1** is of great potential as antitumor candidate for further investigation.

Dual DNA damage mechanism investigation

The title naphthalimide platinum(IV) compounds were purposed to interact with DNA by naphthalimide fragment and the liberated platinum(II) compounds in reducing condition to cause serious DNA injuries to tumor cells. To detect the dual DNA damage mechanism, the DNA interaction properties of compound **1** were investigated by HPLC, electrophoretic dsDNA plasmid method, UV–Vis, and fluorescence assays.

HPLC studies for reduction and DNA interaction of compound 1

The reduction of platinum(IV) to platinum(II) in reducing microenvironment and further binding to DNA is an essential step for the action of platinum(IV) complexes. To validate the reduction potential of the title complexes, compound **1** solution in PBS was incubated and recorded by HPLC with and without reducing agent AsA, which was proven to be present at higher concentrations in tumor cells than in normal tissues. Then guanosine-5′-monophosphate (5′-GMP) was added as a model of DNA base to detect the DNA reacting competence of the liberated platinum(II) complex.

The HPLC results in Fig. S3 demonstrate that compound **1** mainly keeps stable and undergoes no remarkable reduction in PBS in 4 h. The addition of 5′-GMP causes no influence on the stability of platinum(IV) complex in PBS (Fig. S4). Then, compound **1** (500 μM) could be totally reduced in 4 h in the presence of AsA (1 mM) accompanied with the emergences of oxaliplatin and naphthalimide acid peaks (Fig. S5). Moreover, the adduct of oxaliplatin with 5′-GMP (platined-GMP) is observed in the spectra, which demonstrates the conjunction abilities of the liberated platinum(II) compounds with DNA. Accordingly, the HPLC results determine that the title naphthalimide platinum(IV) complex could easily undergo reduction in reducing microenvironment and release platinum(II) complex, which would exert significant DNA damage to tumor cells.

Electrophoretic dsDNA plasmid studies for DNA interaction of compound 1

Nucleic acid electrophoresis is a useful and straightforward analytical technique to monitor the structural variation of DNA. To evaluate the DNA combination properties of title naphthalimide platinum(IV) complex, the electrophoretic dsDNA plasmid assay was applied with plasmid pAUR101 as substrate. The results in Fig. 4 manifest that the plasmid pAUR101 keeps stable in 4 h in buffer (bands a and b). Then, oxaliplatin as positive reference induces a significant shift of the maximum band of pAUR101 after 4 h incubation (bands c and d). Complex **1** could combine with dsDNA plasmid to induce an obvious shift of the covalently closed circular band in 1 h (band e), and further leads total untwisting of supercoiled form to the open circular form in 4 h (band f). Thus, naphthalimide platinum(IV) complex **1** could interact with DNA in tetravalent form which is probably owing to the naphthalimide fragment. Generally, platinum(IV) complexes were regarded to exert fatal DNA damage to tumor cells after reduction to platinum(II) compounds. To detect the DNA interaction properties of the liberated platinum(II) complexes, compound **1** was treated with AsA for 24 h at 37 °C (Comp. **1** + AsA) to allow the platinum(IV) complex totally undergoing reduction to divalent form. It has been proven that AsA could not interact with DNA in buffer solution [24]. Bands g and h demonstrate that the reduced system comp. **1** + AsA could effectively destroy the structure of the dsDNA and convert the supercoil plasmid DNA to the open circular form within 1 h, which is more effective than oxaliplatin and platinum(IV) compound **1**. These results are probably attributed to the synergistic interaction of the liberated platinum(II) and naphthalimide fragments with DNA.

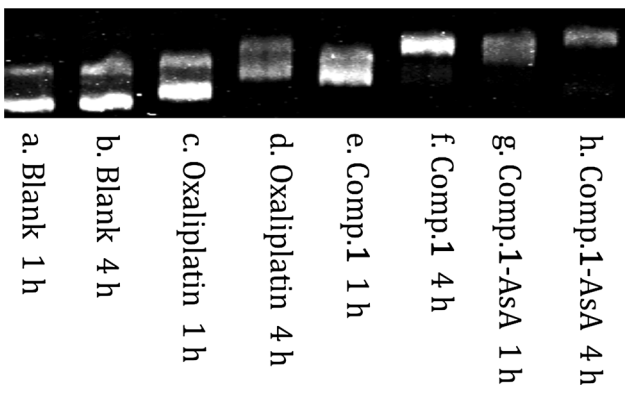

Fig. 4 Electropherograms of dsDNA plasmid pAUR101 incubated with 50 μM of oxaliplatin, platinum(IV) compound **1** or its reduced system comp. **1**-AsA for different incubation time (1 h or 4 h) at 37 °C

UV–Vis studies for DNA interaction of compound 1

The UV–Vis method was widely applied in the detection of the combination of small molecular drugs with DNA [33, 34]. Herein, the calf thymus-DNA (CT-DNA) was selected as a model for UV–Vis experiments to evaluated the DNA binding potential of the naphthalimide platinum(IV) complex. It is observed in Fig. 5 that the absorption of CT-DNA at 260 nm increased gradually with the addition of compound **1** to 24 μM. Moreover, a hypochromic effect is manifested by the observation that the compd. **1**-DNA system exhibits relatively low absorption than the summation of free compound **1** and DNA (compd. **1** + DNA), which is probably attributed to the interaction of the platinum(IV) complex with DNA.

Neutral red (NR) as a planar phenazine dye can bind to DNA by an intercalated mode [35], and was widely employed as a spectral probe to investigate the DNA interaction of drugs. The results in Fig. S1 manifest that CT-DNA could combine with NR to form NR-DNA complex and cause a decrease of the absorption band for NR at 450 nm. Then the competitive interaction of compound **1** and NR with CT-DNA was evaluated and shown in Fig. 6. It could be observed that, with the addition of compound **1** to the NR-DNA system, the absorption at 450 nm improves which reflects the gradual release of NR. It is reasonable to imply that compound **1** could intercalate with CT-DNA via naphthalimide fragment and induce the dissociation of NR-DNA complex.

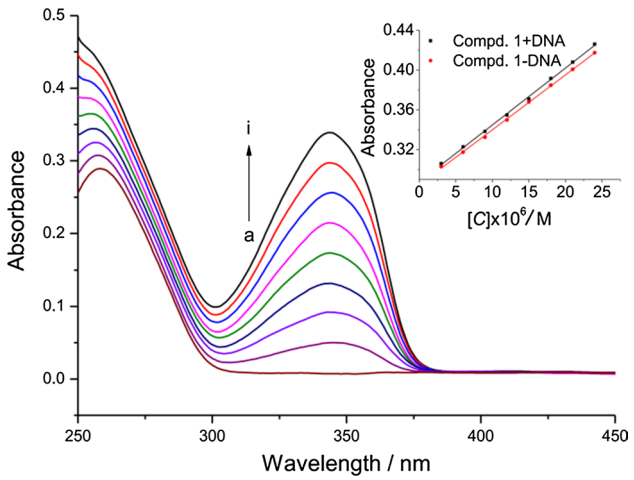

Fig. 5 UV–Vis absorption spectra of CT-DNA (43.0 μM) in the absence and presence of compound **1**. a–i: *c*(compound **1**) = 0.0–24.0 μM with increments of 3.0 μM. Inset: The comparison of absorbance at 260 nm between the compound **1**-DNA complex (compd. **1** − DNA) and the sum values of free compound **1** and free DNA (compd. **1** + DNA)

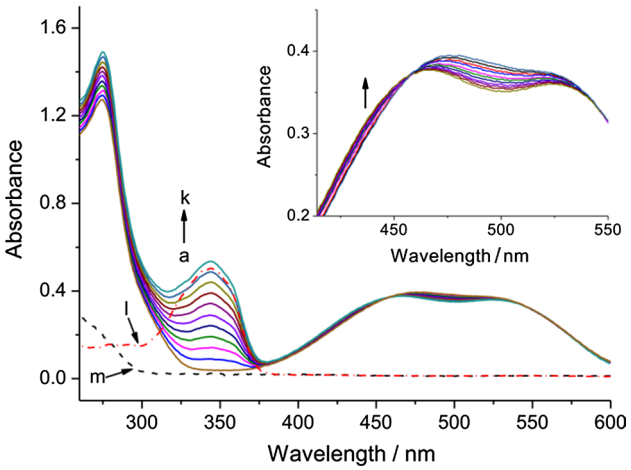

Fig. 6 UV–Vis absorption spectra of NR (40.0 μM) and CT-DNA (43 μM) in the absence and presence of compound **1** (pH 7.4, $T = 298$ K). a–k: *c*(compound **1**) = 0.0–30.0 μM with increments of 3.0 μM; l: spectra of compound **1** (30.0 μM); m: spectra of CT-DNA (43.0 μM)

Fluorescence studies for DNA interaction of compound 1

Further support for the binding of title compound with DNA was obtained through the fluorescence spectra. The results in Fig. 7a indicate that the fluorescence emission of DNA at 505 nm could be quenched by complex **1**, and the quenching trend was in accordance with the Stern–Volmer equation. The Stern–Volmer constant K_{SV} (5.5×10^4 M^{-1}) and quenching constant K_q (5.5×10^{12} M^{-1} s^{-1}) were calculated. It is noticed that the K_q is greater than the maximum scatter collision quenching constant of the biomolecule (2.0×10^{10} M^{-1} s^{-1}) which indicates the probable static quenching procedure. Moreover, platinum(IV) complex **O1** could not induce quenching of the DNA fluorescence emission under the same condition (Fig. S2). Thereby, it is reasonable to deduce that the fluorescence quenching properties of CT-DNA by title naphthalimide platinum(IV) compound is probably owing to the naphthalimide fragment of the title complex rather than the platinum(IV) core, which is in accordance with our literature knowledge. Subsequently, the fluorescence spectra of complex **1** with a fixed concentration (50 μM) were monitored with increasing amount of CT-DNA (0–35 μM) (Fig. 7b). Complex **1** exerts significant fluorescence emission at 399 nm under excitation of 345 nm. With the addition of CT-DNA, the intensity of 399 nm peak increased gradually. Within the investigated concentrations range, the fluorescence increasing the sensitivity of complex **1** is proportional to the concentration of CT-DNA (inset of Fig. 7b), which is probably ascribed to the formation of new complex of the combination of complex **1** with CT-DNA.

Thereby, it is proven that the title complex displays a dual DNA damage mechanism in killing tumor cells. Firstly, the

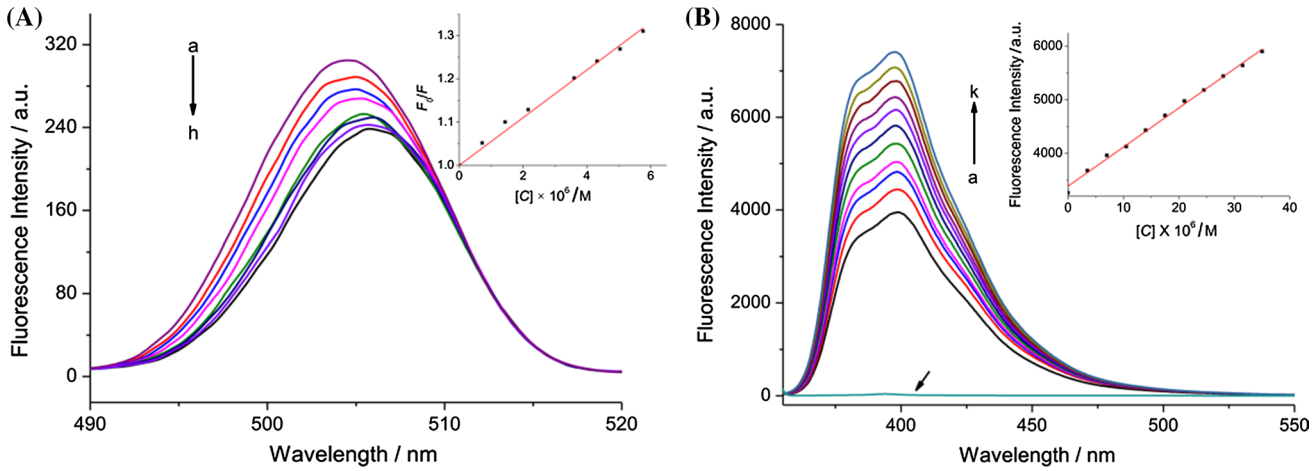

Fig. 7 **a** Fluorescence spectrum of CT-DNA (100 μM) in the absence and presence of the platinum(IV) complex **1** (λ_{ex} = 250 nm, T = 298 K). a–h: c(complex **1**) = 0.00, 0.72, 1.44, 2.16, 3.60, 4.32, 5.04, 5.76 μM. Inset: Stern–Volmer plots for F_0/F vs. $[C] \times 10^6$ of CT-DNA and complex **1** system. **b** Fluorescence spectrum of complex **1** (50 μM) in the absence and presence of the CT-DNA (λ_{ex} = 345 nm, T = 298 K). a–k: c(CT-DNA) = 0.0–35.0 μM at increments of 3.5 μM; l: fluorescence spectrum of free CT-DNA (35.0 μM). Inset: fluorescence intensity at 499 nm with the addition of CT-DNA

naphthalimide platinum(IV) complex would combine with DNA in tetravalent form by naphthalimide ligand and exhibits damage to DNA, which was evidenced by electrophoretic dsDNA plasmid assay, UV–Vis, and fluorescence spectra. Then, the platinum(IV) complex undergoes reduction and releases platinum(II) complex which would intercalate into DNA to cause serious DNA lesion, and this process was proven by HPLC and electrophoretic dsDNA plasmid assays.

Cellular uptake and DNA platination of compound 1

The cellular uptake of chemotherapeutic drugs plays key roles in cancer treatment. The accumulation of platinum drugs in DNA significantly affected their therapeutic effects. The cellular and DNA uptake of naphthalimide platinum(IV) compound **1** was evaluated in SKOV-3 cells with oxaliplatin as a reference drug. The results in Fig. 8 demonstrate that compound **1** accumulates 1.3 folds higher in whole tumor cells than oxaliplatin. Meanwhile, the platination of complex **1** in DNA is 2.8 times higher than the reference drug. The high DNA platination of the title compound is probably a result from the summation of dual DNA interactions of naphthalimide platinum(IV) compounds via naphthalimide fragment and liberated platinum(II) complex in tumor cells.

Apoptosis and western blot

To further detect the action mechanism of the naphthalimide platinum(IV) complex, the apoptosis induction properties of compound **1** was evaluated using oxaliplatin as reference drug by flow cytometry and western blot.

Flow cytometric assay was carried out by an annexin V-FITC and propidium iodide (PI) double-staining method in SKOV-3 cells. The cells were treated with drugs at concentration of 30 μM for 24 h at 37 °C in incubator. The results in Fig. 9 demonstrate that compound **1** could effectively induce apoptosis of SKOV-3 cells (44.71%) in contrast to the blank (8.03%). Furthermore, oxaliplatin promotes

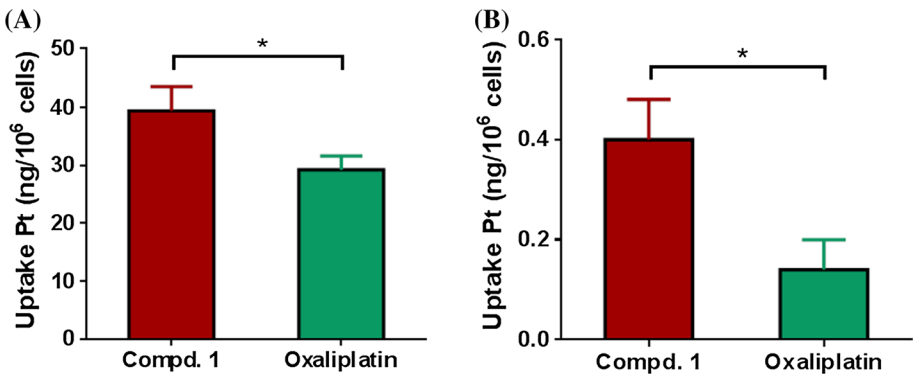

Fig. 8 Cellular uptake and DNA platination of mono naphthalimide platinum(IV) complex **1** and oxaliplatin in SKOV-3 cells. **a** Platinum in whole cells; **b** platinum in DNA

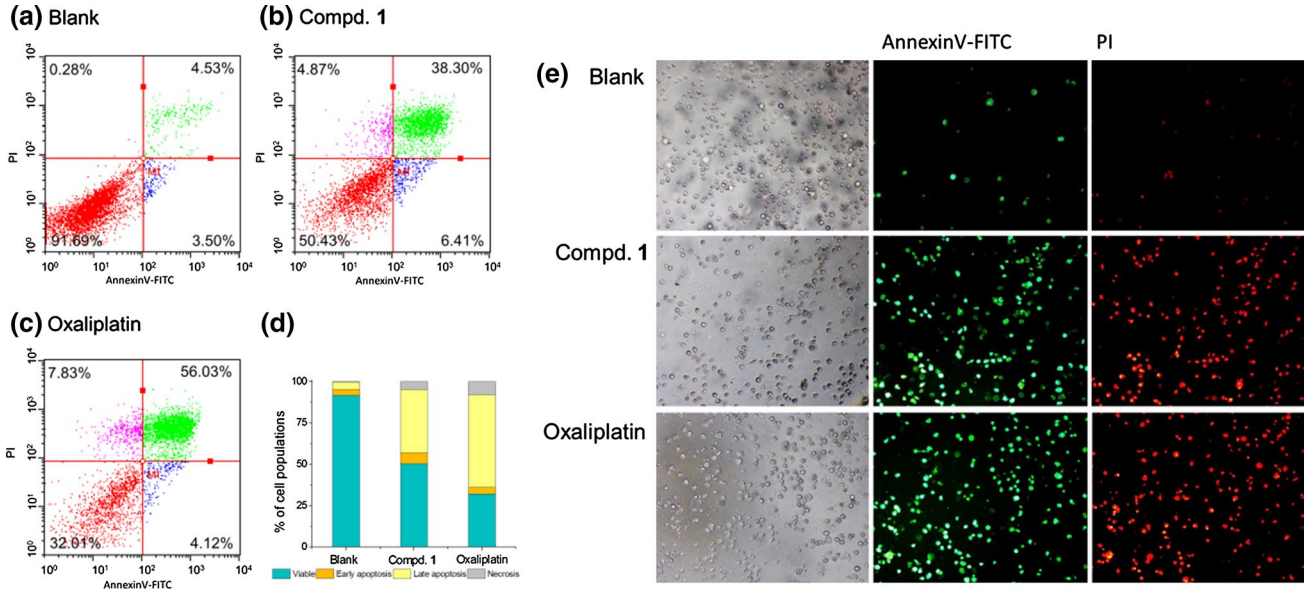

Fig. 9 Apoptosis inducing properties of platinum compounds by annexin V-FITC/PI staining of SKOV-3 cells. SKOV-3 cells were incubated with and without platinum complexes for 24 h at 37 °C. **a** Blank; **b** compound **1** (30 μM); **c** oxaliplatin (30 μM); **d** the stack column; **e** fluorescence microscopic images

larger populations of cells (60.15%) undergoing apoptosis than complex **1**. These facts are probably because of that the activation of platinum(IV) compound **1** is accompanied by reduction to platinum(II) complex, which takes longer time than platinum(II) drug oxaliplatin.

The induction of apoptosis in tumor cells is usually associated with the activation of caspases. Herein, the western blot assay was applied to monitor the influence of the newly prepared complex **1** on the caspase 3/9 in SKOV-3 cells with cisplatin and oxaliplatin as reference drugs. The cells were treated with platinum complexes (20 μM) for 24 h at 37 °C. The expression of caspase 3/9 was tested and afforded in Fig. 10. Exposure of SKOV-3 cells to compound **1** induces high expression of caspase 3/9 as well as cleaved-caspase 3 in contrast to the untreated group (blank) which is similar to that of reference platinum(II) drugs cisplatin and oxaliplatin. These observations prove that compound **1** might cause apoptosis of SKOV-3 cells via an intrinsic apoptosis pathway.

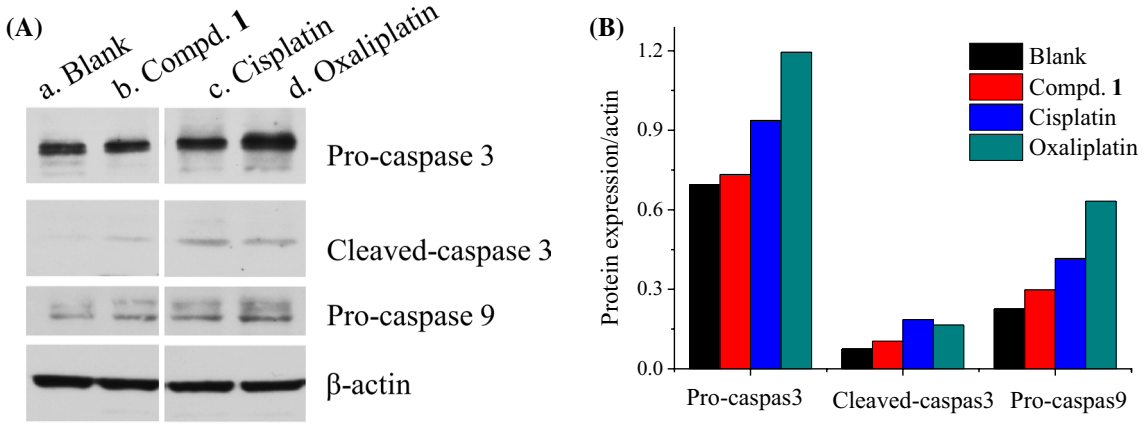

Fig. 10 Cell apoptotic pathway western blot analysis of SKOV-3 cells incubated with and without compound **1**, cisplatin and oxaliplatin. SKOV-3 cells were incubated with and without platinum complexes for 24 h at 37 °C (blank: no compound; cisplatin, oxaliplatin, compound **1**: 20 μM). **a** Blots. **b** Relative gray intensity analysis [relative gray intensity = (gray intensity of indicated protein)/(gray intensity of *β*-actin)]

HSA binding studies of compound 1

HSA as the main transporter protein in human circulating blood plays a key role in the storage and transportation of numerous exogenous drugs and would further influence their pharmacokinetic and pharmacodynamic properties like biodistribution, solubility, half-life in the body, metabolism, etc. [36, 37]. Notably, the complexation of small drug with HSA possesses many properties of nanoparticle drugs and would favour the drug targeting tumor cells via the enhanced permeability and retention (EPR) effect [38]. Thus, it is of rational and fundamental importance to investigate the combination of drugs with HSA.

The fluorescence spectra in Fig. 11 manifest that the HSA exerts significant emission peak at 343 nm under excitation of 280 nm (line a), meanwhile complex **1** displays no significant emission at such wavelength (line l). The results demonstrate that the emission of HSA quenches gradually with the addition of complex **1** from 0.0 μM to 12.5 μM (lines a–k), accompanied with a blue shift of maximum emission wavelength from 343 to 337 nm.

Then, to detect the quenching mechanism, the quenching spectra of HSA with complex **1** at different temperatures (298 K, 304 K, and 307 K) were recorded (Fig. 11 and S7). The quenching trends at three temperatures are all in agreement with the linear Stern–Volmer equation. Then, the Stern–Volmer constants K_{SV}, quenching constants K_q, binding constants K_b, number of binding sites n, and the thermodynamic parameters for compound **1**-HSA system are calculated and the detail calculation procedure was supplied in ESI.

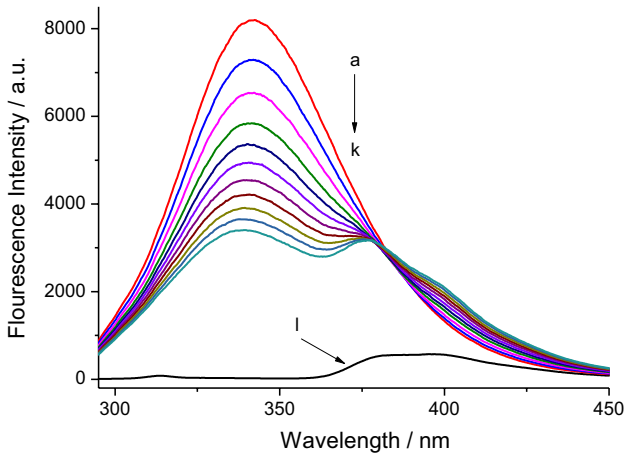

Fig. 11 Fluorescence spectra of HSA in the absence and presence of the platinum(IV) complex **1** (λ_{ex} = 280 nm, T = 298 K). a–k: c(HSA) = 4.0 μM, c(complex **1**) = 0.0–12.5 μM, at increments of 1.25 μM; l: fluorescence spectrum of free complex **1**, c(complex **1**) = 12.5 μM

It is demonstrated that the Stern–Volmer constants K_{SV} and binding constants K_b are inversely correlated with temperature, and the quenching constants K_q are higher than the maximum scatter collision quenching constant of the biomolecule, which indicate that the quenching procedure of HSA by complex **1** is probably a static quenching process. The binding sites n of compound **1** with HSA are approximately equal to 1, demonstrating that platinum(IV) complex **1** could combine with HSA by one affinity binding site. The thermodynamic parameters are calculated by van't Hoff equation. It has been manifested that the sign and magnitude of the thermodynamic parameter are associated with various individual kinds of interaction that may take place in protein association processes. From the thermodynamic standpoint, $\Delta H > 0$ and $\Delta S > 0$ imply a hydrophobic interaction, $\Delta H < 0$ and $\Delta S < 0$ reflect the van der Waals force or hydrogen bond formation, and $\Delta H < 0$ and $\Delta S > 0$ are characteristics for electrostatic interactions. The negative Gibbs free energy change ΔG evidences the spontaneous combination of compound **1** with HSA. Then the negative enthalpy change ΔH and entropy change ΔS prove that such process is mainly driven by enthalpy, and the hydrogen bond and van der Waals force are probably involved in the interaction of HSA with compound **1**.

Subsequently, the UV–Vis method was also employed to confirm the combination of HSA with compound **1**. The UV–Vis spectra in Fig. S11 reveal that the absorbance of HSA is not superposed with the subtracting spectrum of the mixed compound **1**-HSA system and compound **1** in the range of 250–300 nm. These facts offer new proofs for the interaction of compound **1** with HSA [39].

Accordingly, the results from fluorescence and UV–Vis spectra disclose the spontaneous interaction of naphthalimide platinum(IV) complex with HSA, which would further influence their transport and storage as well as action in organism.

Conclusion

In conclusion, a series of new mono naphthalimide platinum(IV) complexes with oxaliplatin core were designed, prepared, and evaluated for antitumor activities in vitro and in vivo. The title complexes inhibit the proliferation of all tested tumor cell lines in vitro and possess much potential in overcoming drug resistance of cisplatin. The linker between the naphthalimide and platinum(IV) core displays great influence on the bioactivities. Especially, complex **1** with propionyl chain exerts the most prominent antitumor activities, which is more prominent than its precursor oxaliplatin, and comparable to cisplatin. Then, the modification of naphthalimide with nitro moiety also exerts much influence on antitumor

activities. Moreover, the in vivo antitumor evaluation demonstrates that compound **1** exerts promising tumor growth inhibitory competence against CT26 xenograft tumors in BALB/c without inducing severe toxic effects on the mice. The mechanism detection proves that the title complexes exhibit a dual DNA damage mechanism. The naphthalimide platinum(IV) complex could intercalate into DNA by naphthalimide group and causing dysfunction of DNA, meanwhile the liberated platinum(II) after reduction induces a remarkable secondary nuclear damage to tumor cells. The synergetic action mechanism could active the apoptotic pathway of tumor cells by up-regulating the expression of apoptotic proteins caspase 9 and caspase 3. Moreover, the transformation of platinum(II) drug into tetravalent form by introducing naphthalimide remarkably increases the uptake of platinum in whole cells and DNA simultaneously. All these facts may be the factors for the synthesized platinum(IV) complexes to overcome the resistance of cisplatin. Besides, naphthalimide platinum(IV) complex could interact with HSA by hydrogen bond and van der Waals force which would further influence their storage, transport, and bioactivities. Accordingly, the title naphthalimide platinum(IV) derivatives reported here pending with mono naphthalimide moiety are of prime significance for further development as effective antitumor agents.

Experimental

All reactions were carried out under an atmosphere of nitrogen in flame-dried glassware with magnetic stirring unless otherwise indicated. Cisplatin and oxaliplatin were purchased from Yurui chemical Co. Ltd. (Shanghai, China). Other reagents were obtained from Alfa Aesar, Sigma, Aladdin, and J&K Scientific Ltd. ^{1}H NMR and ^{13}C NMR spectra were recorded on a Varian (400 MHz and 100 MHz). All NMR chemical shifts were referenced to residual solvent peaks or TMS as an internal standard. All coupling constants *J* were quoted in Hz. High-resolution mass spectra (HRMS) were obtained on an IonSpec QFT mass spectrometer with ESI ionization. The HPLC analyses were performed on a Thermo Ultimate 3000 RS equipped with an Agilent Eclipse XDB-C18 column (250 × 4.6 mm, 5 μm). The plasmid pAUR101 was purchased from Takala. The HSA was purchased from Sigma. Genomic DNA mini preparation kit and annexin V-FITC/PI apoptosis detection kit were purchased from Beyotime, China. UV–Vis spectra were measured on a Scinco S-3100 UV–Vis spectrophotometer. Fluorescence spectroscopic data were recorded on a Hitachi F-7000 spectrofluorometer. Flow cytometry was performed on a Millipore Guava easyCyte 8HT flow cytometer.

Chemistry

The synthetic procedures of acids **A1**–**A4** and oxoplatin **O1** are given in supporting information according to procedures mentioned in literature.

3-(1,3-Dioxo-1*H*-benzo[*de*]isoquinolin-2(3*H*)-yl)propanoyl oxalato (*trans*-(-)-1,2-cyclohexanediamine) chloro platinum(IV) (1, $C_{23}H_{24}ClN_3O_8Pt$) To a solution of 78 mg compound **A-1** (0.29 mmol) and 94 mg TBTU (0.29 mmol) in 5 cm^3 dry DMF was injected 40 mm^3 TEA (0.29 mmol), and the mixture was allowed to intensively stir for 10 min at room temperature. Then 100 mg oxoplatin (0.20 mmol) was added and the reaction mixture was stirred for another 48 h at 50 °C. The solvent was evaporated, and the residue was purified by silica gel column chromatography to afford compound **1** as white solid (36 mg, 25%). M.p.: 214–216 °C; ^{1}H NMR (400 MHz, DMSO-d_6): δ = 8.52–8.42 (m, 4H, naphthalimide-*H*), 7.89 (d, *J* = 7.6 Hz, 2H, naphthalimide-*H*), 4.24 (s, 2H, N-CH_2), 2.71–2.57 (m, 4H, N-CH$_2$CH_2, cyclohexyl C*H*), 2.06 (dd, *J* = 30.6, 11.5 Hz, 2H, cyclohexyl, CH_2), 1.45 (dd, *J* = 44.3, 8.8 Hz, 4H cyclohexyl, CH_2), 1.15 (s, 2H, cyclohexyl CH_2) ppm; ^{13}C NMR (100 MHz, DMSO-d_6): δ = 178.39 (PtO*C*=OCH$_2$), 163.83 (oxaliplatin *C*=O), 163.76 (naphthalimide 1,8-*C*=O), 134.80 (naphthalimide 4,5-*C*), 131.74 (naphthalimide 12-*C*), 131.11 (naphthalimide 2,7-*C*), 127.84 (naphthalimide 11-*C*), 127.65 (naphthalimide 3,6-*C*), 122.55 (naphthalimide 9,10-*C*), 62.01 (oxaliplatin *C*H), 61.47 (oxaliplatin *C*H), 36.75 (N-*C*H$_2$), 35.12 (N-CH$_2$*C*H$_2$), 31.30 (oxaliplatin *C*H$_2$), 31.04 (oxaliplatin *C*H$_2$), 24.03 (oxaliplatin *C*H$_2$), 23.97 (oxaliplatin *C*H$_2$) ppm; HRMS: *m/z* calcd. 701.0972 ([M+H]$^+$), found 701.0955; IR (KBr): $\bar{\nu}$ = 3444, 3270, 3074 (Ar–H), 2921 (CH$_2$, NH$_2$), 1695, 1613 (C=O), 1557, 1507, 1426 (aromatic frame), 1392, 1329, 1269, 1207, 1152, 1080, 853, 814 cm^{-1}.

4-(1,3-Dioxo-1*H*-benzo[*de*]isoquinolin-2(3*H*)-yl)butanoyl oxalato (*trans*-(-)-1,2-cyclohexanediamine) chloro platinum(IV) (2, $C_{24}H_{26}ClN_3O_8Pt$) To a solution of 82 mg compound **A-2** (0.29 mmol) and 94 mg TBTU (0.29 mmol) in 5 cm^3 dry DMF was injected 40 mm^3 TEA (0.29 mmol), and the mixture was allowed to intensively stir for 10 min at room temperature. Then 100 mg oxoplatin (0.20 mmol) was added and the reaction mixture was stirred for another 48 h at 50 °C. The solvent was evaporated, and the residue was purified by silica gel column chromatography to afford compound **2** as white solid (39 mg, 27%). M.p.: 192–194 °C; ^{1}H NMR (400 MHz, DMSO-d_6): δ = 8.51 (d, *J* = 7.1 Hz, 2H, naphthalimide-*H*), 8.40 (d, *J* = 8.0 Hz, 2H, naphthalimide-*H*), 7.84 (t, *J* = 7.6 Hz, 2H, naphthalimide-*H*), 4.26–3.98 (m, 2H, N-CH_2), 3.26–2.61 (m, 2H, cyclohexyl C*H*), 2.41–2.35 (m, 2H, COCH_2), 2.20 (d, *J* = 12.1 Hz, 1H, cyclohexyl CH_2), 1.88–1.96 (m, 3H, cyclohexyl CH_2, N-CH$_2$CH_2), 1.56 (s,

4H, cyclohexyl CH_2), 1.22 (d, J = 7.1 Hz, 2H, cyclohexyl CH_2) ppm; ^{13}C NMR (100 MHz, DMSO-d_6): δ = 180.71 (PtO*C*=OCH_2), 163.98 (oxaliplatin *C*=O), 163.59 (naphthalimide 1,8-*C*=O), 134.77 (naphthalimide 4,5-*C*), 131.71 (naphthalimide 12-*C*), 131.17 (naphthalimide 2,7-*C*), 127.82 (naphthalimide 11-*C*), 127.66 (naphthalimide 3,6-*C*), 122.47 (naphthalimide 9,10-*C*), 61.72 (2C, oxaliplatin *C*H), 46.12 (N-*C*H_2), 34.11 (N-CH_2CH_2*C*H_2), 31.36 (oxaliplatin *C*H_2), 31.14 (oxaliplatin *C*H_2), 24.24 (N-CH_2*C*H_2), 24.00 (oxaliplatin *C*H_2), 23.86 (oxaliplatin *C*H_2) ppm; HRMS: *m/z* calcd. 715.1129 ([M+H]$^+$), found 715.1107; IR (KBr): $\bar{\nu}$ = 3450, 3250, 3080 (Ar–H), 2932 (CH_2, NH_2), 1700, 1680 (C=O), 1610, 1556, 1510, 1420 (aromatic frame), 1390, 1370, 1290, 1200, 1150, 1080, 839, 803 cm^{-1}.

5-(1,3-Dioxo-1*H*-benzo[*de*]isoquinolin-2(3*H*)-yl)pentanoyl oxalato (*trans*-(-)-1,2-cyclohexanediamine) chloro platinum(IV) (3, $C_{25}H_{28}ClN_3O_8Pt$) To a solution of 86 mg compound **A-2** (0.29 mmol) and 94 mg TBTU (0.29 mmol) in 5 cm^3 dry DMF was injected 40 mm^3 TEA (0.29 mmol), and the mixture was allowed to intensively stir for 10 min at room temperature. Then 100 mg oxoplatin (0.20 mmol) was added and the reaction mixture was stirred for another 48 h at 50 °C. The solvent was evaporated, and the residue was purified by silica gel column chromatography to afford compound **3** as white solid (38 mg, 26%). M.p.: 210–212 °C; ^{1}H NMR (400 MHz, DMSO-d_6): δ = 8.50–8.43 (m, 4H, naphthalimide-*H*), 7.87 (t, J = 7.7 Hz, 2H, naphthalimide-*H*), 4.14–4.00 (m, 2H, NCH_2), 3.18–2.57 (m, 2H, cyclohexyl C*H*), 2.35 (t, J = 7.1 Hz, 2H, CO-CH_2), 2.00–2.10 (m, 2H, cyclohexyl CH_2), 1.70–1.39 (m, 7H, cyclohexyl CH_2, N-CH_2CH_2), 1.37–1.03 (m, 3H, cyclohexyl CH_2, CO-CH_2CH_2) ppm; ^{13}C NMR (100 MHz, DMSO-d_6): δ = 181.17 (PtO*C*=OCH_2), 163.83 (oxaliplatin *C*=O), 163.58 (naphthalimide 1,8-*C*=O), 134.73 (naphthalimide 4,5-*C*), 131.72 (naphthalimide 12-*C*), 131.14 (naphthalimide 2,7-*C*), 127.78 (naphthalimide 11-*C*), 127.64 (naphthalimide 3,6-*C*), 122.47 (naphthalimide 9,10-*C*), 62.00 (2C, oxaliplatin *C*H), 61.87 (N*C*H_2), 49.04 (CO*C*H_2), 36.63 (NCH_2*C*H_2), 31.35 (oxaliplatin *C*H_2), 31.03 (oxaliplatin *C*H_2), 27.57 (COCH_2*C*H_2), 23.93 (oxaliplatin *C*H_2), 23.34 (oxaliplatin *C*H_2) ppm; HRMS: *m/z* calcd. 729.1285 ([M+H]$^+$), found 729.1262; IR (KBr): $\bar{\nu}$ = 3450, 3219 (Ar–H), 2927 (CH_2, NH_2), 1728, 1616 (C=O), 1559, 1512, 1424 (aromatic frame), 1388, 1362, 1257, 1201, 1147, 1078, 850, 813 cm^{-1}.

4-(5-Nitro-1,3-dioxo-1*H*-benzo[*de*]isoquinolin-2(3*H*)-yl)-butanoyl oxalato (*trans*-(-)-1,2-cyclohexanediamine) chloro platinum(IV) (4, $C_{24}H_{25}ClN_4O_{10}Pt$) To a solution of 95 mg compound **A-2** (0.29 mmol) and 94 mg TBTU (0.29 mmol) in 5 cm^3 dry DMF was injected 40 mm^3 TEA (0.29 mmol), and the mixture was allowed to intensively stir for 10 min at room temperature. Then 100 mg oxoplatin (0.20 mmol) was added and the reaction mixture was stirred for another 48 h at 50 °C. The solvent was evaporated, and the residue was purified by silica gel column chromatography to afford compound **4** as white solid (42 mg, 27%). M.p.: 181–183 °C; ^{1}H NMR (400 MHz, DMSO-d_6): δ = 9.46 (d, J = 2.2 Hz, 1H, naphthalimide 5-*H*), 8.93 (d, J = 2.2 Hz, 1H, naphthalimide 4-*H*), 8.76 (d, J = 8.0 Hz, 1H, naphthalimide 2-*H*), 8.65 (d, J = 6.4 Hz, 1H, naphthalimide 7-*H*), 8.05 (t, J = 7.8 Hz, 1H, naphthalimide 3-*H*), 4.05–4.15 (m, 2H, NCH_2), 2.73 (s, 1H, cyclohexyl C*H*), 2.61 (s, 1H, cyclohexyl C*H*), 2.38 (t, J = 7.4 Hz, 2H, COCH_2), 2.17–2.04 (m, 2H, cyclohexyl CH_2), 1.93–1.84 (m, 2H, cyclohexyl CH_2), 1.64–1.37 (m, 4H, NCH_2CH_2, cyclohexyl CH_2), 1.27–1.13 (m, 2H, cyclohexyl CH_2) ppm; ^{13}C NMR (100 MHz, DMSO-d_6): δ = 180.77 (PtO*C*=OCH_2), 163.55 (oxaliplatin *C*=O), 163.35 (naphthalimide 1-*C*=O), 162.88 (naphthalimide 8-*C*=O), 146.23 (naphthalimide 3-*C*), 136.72 (naphthalimide 4-*C*), 134.33 (naphthalimide 2-*C*), 131.26 (naphthalimide 5-*C*), 130.09 (naphthalimide 12-*C*), 129.66 (naphthalimide 7-*C*), 127.65 (naphthalimide 11-*C*), 124.47 (naphthalimide 6-*C*), 123.31 (naphthalimide 9-*C*), 123.06 (naphthalimide 10-*C*), 61.89 (oxaliplatin *C*H), 61.79 (oxaliplatin *C*H), 34.00 (N-*C*H_2), 31.39 (N-CH_2CH_2*C*H_2), 31.15 (2C, oxaliplatin *C*H_2), 24.07 (N-CH_2*C*H_2), 23.91 (2C, oxaliplatin *C*H_2) ppm; HRMS: *m/z* calcd. 760.0980 ([M+H]$^+$), found 760.0961; IR (KBr): $\bar{\nu}$ = 3444, 3199 (Ar–H), 2939, 2860 (CH_2, NH_2), 1727, 1612 (C=O), 1560, 1512, 1445 (aromatic frame), 1388, 1367, 1278, 1200, 1147, 1078, 1025, 850, 809 cm^{-1}.

In vitro cellular cytotoxicity assays

All the platinum(IV) derivatives **1**–**4** were evaluated for antitumor activities against ovarian cancer (SKOV-3), cervical cancer (HeLa), lung cancer (A549), and cisplatin-resistant cell A549R, and murine colon cancer (CT26) as well as human embryonic kidney cell (293T) using a 3-(4,5-dimethylthiazol-2-yl)-2,5-diphenyltetrazolium bromide (MTT) assay. Dulbecco's Modified Eagle Medium (DMEM), RPMI1640, 0.25% trypsin/EDTA solutions, fetal bovine serum (FBS), and penicillin–streptomycin solutions were purchased from Gibco. MTT was purchased from Sigma. The cells were maintained in either DMEM (for HeLa, 293T cells) or RPMI1640 (for SKOV-3, A549, A549R, CT26 cells) medium containing 10% FBS in a humidified atmosphere containing 5% CO_2 at 37 °C. The A549R was maintained with 2 μg/cm^3 cisplatin. Phosphate buffered saline (PBS) contained 137 mM NaCl, 2.7 mM KCl, 10 mM Na_2HPO_4, and 2 mM KH_2PO_4 (pH 7.4). MTT solution at concentration of 5 mg/cm^3 for MTT assays was prepared before it used.

Cells were seeded in 96-well plates at 5000 cells per well in 100 mm^3 of complete medium and incubated for 24 h in a 5% CO_2 atmosphere at 37 °C. Then freshly prepared culture

medium 100 mm^3 containing drugs at different concentrations (100 μM, 45.9 μM, 21.1 μM, 9.7 μM, 4.5 μM, 2.0 μM, 0.9 μM, 0.4, and 0.0 μM) were added. The cells were further incubated for another 48 h. After that, freshly prepared MTT solution (5 mg/cm^3) 20 mm^3 was added. The resultant mixtures were incubated for 4 h to allow viable cells to reduce the yellow tetrazolium salt into dark blue formazan crystals. After removal of the medium, formazan was dissolved in DMSO (150 mm^3) and quantified by a microplate reader (570 nm). The IC_{50} values were calculated using GraphPad Prism 6 based on three parallel experiments.

In vivo antitumor assay

BALB/c mice (18–20 g) were purchased from the Laboratory Animal Center, Shandong University (Shandong, China). All animals received care in compliance with the guidelines outlined in the National Institutes of Health guide for the care and use of Laboratory animals (NIH Publications No. 8023, revised 1978).

Murine CT26 cells (5×10^5) were injected subcutaneously into the right flank of male BALB/c mice and therapy was started when tumor nodules were palpable (day 6). The mice were divided into three groups randomly, NaCl group; oxaliplatin group (5 mg Pt per kg); compound **1** group (5 mg Pt per kg). Freshly prepared solutions of drugs were administered i.p. for five times at 3 days intervals on days 6, 9, 12, 15, and 18. Tumor growth was assessed by measuring the perpendicular diameter of the tumor using calipers. The mice were killed after 24 h of the last drug application (day 19) and the tumors were excised and weighed. The blood and tissues including heart, lung, liver, spleen, and kidney were collected. Samples for histological evaluation were formalin-fixed and paraffin-embedded. H&E stains were performed by standard procedures.

Electrophoretic dsDNA plasmid assay

The pAUR101 plasmid dsDNA (6687 bp) was applied for electrophoretic assay as a model of dsDNA. The DNA interaction reactions were performed in PBS buffer. Platinum(IV) complex **1** was evaluated for DNA binding properties with cisplatin and oxaliplatin as positive DNA intercalators. Moreover, to detect the influence of reduction of platinum(IV) complex on the DNA binding properties, the reduced system (compd. **1**-AsA) of compound **1** (1 mM) was prepared in the presence of AsA (5 mM) after incubation at 37 °C for 48 h. Then the resultant solution was diluted for 20 folds and used in the electrophoretic assay.

Solutions a-h containing plasmid DNA 20 mm^3 were added platinum complexes (a, b: blank; c, d: oxaliplatin, 50 μM; e, f: compound **1**, 50 μM; g, h: Compound 1-AsA, 50 μM). The resultant mixtures a, c, e, g were incubated at 37 °C by a thermo cycler for 1 h, and mixtures b, d, f, h were incubated for 4 h. Then, the samples were loaded in the agarose gel (1.0% w/v) and electrophoresis was carried out in TAE 1× (Tris–acetate-EDTA) buffer for a period of 30 min at approximately 150 V. Subsequently, the gel was stained with Gel Red for 30 min, and imaged with a Bio-Rad Universal Hood II instrument.

UV–Vis spectra assays for DNA binding

To investigate the DNA interaction of title compounds, CT-DNA was used as a model of DNA. The experiments were carried out in Tris–HCl buffer (10 mM Tris–HCl/10 mM NaCl, pH 7.4). The UV–Vis absorbance was recorded from 200 to 800 nm using a quartz cell of path length 1 cm at room temperature with a scan rate of 600 nm min^{-1}.

Compound **1** was added to DNA solution (43.0 μM) gradually with concentrations raising from 0.0 to 24.0 μM at increments of 3.0 μM, and the UV–Vis spectra were tested. Then the UV–Vis spectrum of free complex **1** was also recorded.

NR was applied in the detection of the DNA interaction of compound **1**. The UV–Vis spectra of NR in the absence and presence of CT-DNA (pH 7.4, $T = 298$ K) were tested by the addition of CT-DNA in concentrations of 0.0–43.0 μM with increments of 4.3 μM to the NR solution (40.0 μM). The spectra were given as Fig. S1. Then, to the NR-DNA solution containing NR (40.0 μM) and CT-DNA (43.0 μM) was added compound **1** (0.0–30.0 μM with increments of 3.0 μM). The absorption spectra were recorded and given as Fig. 6 to evidence the competitive intercalation of complex **1** and NR with CT-DNA.

Fluorescence spectra assays for DNA binding

The fluorescence spectra were carried out in buffer solution (10 mM Tris–HCl/10 mM NaCl, pH 7.4) on a Hitachi F-7000 spectrofluorometer using a quartz cell of 1.00 cm. To the CT-DNA solution (100 μM) was added platinum(IV) complex **1** or **O1** gradually and the spectra were recorded from 260 to 800 nm at a scan rate of 300 nm min^{-1} under excitation of 250 nm at 298 K. The widths of both the excitation and emission slits were 5.0 nm.

The fluorescence spectrum of complex **1** (50.0 μM) in the absence and presence of the CT-DNA (0.0–35.0 μM at increments of 3.5 μM) were prepared. The spectra were recorded from 350 to 800 nm at a scan rate of 300 nm min^{-1} under excitation of 345 nm at 298 K and given as Fig. 7. The fluorescence spectrum of free CT-DNA (35.0 μM) was also tested. The widths of both the excitation and emission slits were 5.0 nm.

HPLC assay for DNA binding

The reduction of platinum(IV) complex by AsA and the DNA binding properties of the liberated platinum(II) complex were testified using a HPLC assay. The HPLC was assessed on Thermo Ultimate 3000 RS equipped with an Agilent Eclipse XDB-C18 column (250 × 4.6 mm, 5 μm). HPLC profiles were recorded by a diode array detector with flow rate of 1 cm^3/min. The linear gradient was given in Table 2.

The solution of compound **1** (500 μM) in PBS was prepared and monitored for 15 h to evaluate its stability in solution (Fig. S3). Then, the reduced potential of platinum(IV) compound **1** was confirmed in the presence of AsA (1 mM, similar concentration as in tumor cells). 5′-GMP was applied as a model of DNA base. The solution containing compound **1** (500 μM), 5′-GMP (3 mM) and AsA (1 mM) was tested to evaluate the degradation of compound **1** by AsA and the following combination with 5′-GMP of the liberated platinum(II) complex (Fig. S5). The solution of compound **1** (500 μM) in the presence of 5′-GMP (3 mM) without AsA was also tested as a negative experiment (Fig. S4).

Cell uptake and DNA platination

The SKOV-3 cells were seeded in 6-well cell culture plate and incubated for 12 h in incubator. Then platinum drugs (50 μM) were added and the cells were treated with drugs for 12 h. After that, all cells were harvested and washed with PBS (1 $cm^3 \times 3$) to remove the residue drugs. The cells were counted with an Invitrogen countess II automated cell counter and then mineralized with 70% HNO_3 (LC). The cellular uptake were quantitative analyzed by ICP-MS. Cellular platinum levels were expressed as ng Pt per million cells and the results were achieved as a mean of three determinations for each data point.

For DNA platination, ca. 1 million SKOV-3 cells after treatment mentioned above were extracted with a Genomic DNA Mini Preparation Kit, and the DNA were mineralized with 70% HNO_3. The platinum in DNA was evaluated by ICP-MS.

Table 2 The linear gradient for HPLC

Time/min	A (0.1% aqueous TFA)/%	B (Methol)/%
0	90	10
5	90	10
35	0	100
45	0	100

Apoptosis experiments–Annexin V/PI assay

The apoptosis experiments were performed according to the manufacture's protocol (Beyotime Biotechnology Annexin V-FITC/PI apoptosis detection kit, Beyotime Biotechnology). SKOV-3 cells were incubated with or without the test compounds for 24 h at 37 °C (blank: no compound; compound **1**: 30 μM; oxaliplatin: 30 μM). Then the cells were harvested from adherent cultures by trypsinization with no EDTA. Following centrifugation at 1000 rpm for 5 min, cells were washed with PBS twice and suspended in binding buffer 200 mm^3. Subsequently, the samples were stained with annexin V-FITC 5 mm^3 and PI 10 mm^3 for 15 min at room temperature and tested by flow cytometric assay. Following that, the samples were imaged with a fluorescence microscope (Nikon) under visible light, blue light, and green light, respectively.

Western blot method

The influence of platinum(IV) complexes **1**, cisplatin, and oxaliplatin on the expression of the apoptotic proteins caspase 3/9 were evaluated. The SKOV-3 cells were treated with or without platinum compounds for 24 h in incubator (blank: no compound; cisplatin, oxaliplatin, compound **1**: 20 μM). Proteins were extracted with lysis buffer, and their concentrations were measured by bicinchoninic acid (BCA) assay using a BCA protein assay kit (Servicebio). The proteins (20 mg/lane) were separated by 10% sodium dodecyl sulfate–polyacrylamide gel electrophoresis (SDS-PAGE) (Servicebio) and transferred onto polyvinylidene difluoride (PVDF) Immobilon-P membrane (Millipore). The β-actin was used as a loading control. The blots were blocked with 5% nonfat milk in TBST (Trisbuffered saline plus 0.1% Tween 20) for 1 h. The membrane was incubated with primary antibodies overnight at 4 °C. Then, the membrane was washed with PBST for three times and incubated with secondary antibody for 1 h at 37 °C. After that, the membrane was treated with an ECL western blotting substrate kit (Servicebio) and detected by a scanning system (EPSON).

Fluorescence spectra assays for HSA binding

The fluorescence quenching spectra of HSA by compound **1** was recorded by the addition of compound **1** (0.0–12.5 μM, at increments of 1.25 μM) gradually to the HSA solution (4.0 μM). The fluorescence spectrum of compound **1** was tested. The quenching spectra at 298 K, 304 K, and 307 K were also recorded. The experiments were performed in buffer solution (10 mM Tris–HCl/10 mM NaCl, pH 7.4) on a Hitachi F-7000 spectrofluorometer using a quartz cell of 1.00 cm. The widths of both the excitation and emission slits were 5.0 nm. The well-mixed solutions were holding

for 15 min for equilibrium, and the fluorescence emission spectra under excitation of 280 nm were tested from 290 to 500 nm at a scan rate of 300 nm min^{-1}.

UV–Vis spectra assays for HSA binding

The UV–Vis spectra were recorded on a Hitachi U-3900H UV–Vis spectrophotometer. The experiments were carried out in Tris–HCl buffer (10 mM Tris–HCl/10 mM NaCl, pH 7.4) at room temperature. The UV–Vis absorbance was recorded from 200 to 600 nm using a quartz cell of path length 1 cm at room temperature with a scan rate of 600 nm min^{-1}. The absorption spectrum (line B) of compound **1**-HSA system (c(HSA) = 10 μM, c(compound **1**) = 15 μM) was recorded. The UV–Vis spectra of free HSA (10 μM) (line A) and compound **1** (15 μM) (line C) were also tested. Then, the subtracting spectrum of line B and line C were calculated and drawn as line D to compare with line A.

Acknowledgements The work was supported by National Natural Science Foundation of China (No. 21807056), Natural Science Foundation of Shandong (No. ZR2017BH092), Doctoral Foundation of Liaocheng University (No. 318051635), Open Project of Shandong Collaborative Innovation Center for Antibody Drugs (No. CIC-AD1836, CIC-AD1835), National Science and Technology Major Project of China (No. 2017ZX09201-003) and Taishan Scholar Research Foundation. This work was also technically supported by Shandong Collaborative Innovation Center for Antibody Drugs and Engineering Research Center for Nanomedicine and Drug Delivery Systems.

References

1. Bray F, Ferlay J, Soerjomataram I, Siegel RL, Torre LA, Jemal A (2018) CA Cancer J Clin 68:394
2. Allemani C, Matsuda T, Carlo DV, Harewood R, Matz M, Nikšić M, Bonaventure A, Valkov M, Johnson CJ, Estève J, Ogunbiyi OJ, Silva GA, Chen WQ, Eser S, Engholm G, Stiller CA, Monnereau A, Woods RR, Visser O, Lim GH, Aitken J, Weir HK, Coleman MP (2018) Lancet 391:1023
3. Wong E, Christen MG (1999) Chem Rev 99:2451
4. Allardyce CS, Dyson PJ (2016) Dalton Trans 45:3201
5. Wheate NJ, Walker S, Craig GE, Oun R (2010) Dalton Trans 39:8113
6. Oun R, Mouss YE, Wheate NJ (2018) Dalton Trans 47:6645
7. Johnstone TC, Suntharalingam K, Lippard SJ (2016) Chem Rev 116:3436
8. Gibson D (2016) Dalton Trans 45:12983
9. Schreiber-Brynzak E, Pichler V, Heffeter P, Hanson B, Theiner S, Lichtscheidl-Schultz I, Kornauth C, Bamonti L, Dhery V, Groza D, Berry D, Berger W, Galanski M, Jakupec MA, Keppler BK (2016) Metallomics 8:422
10. Tan XX, Li GS, Wang QP, Wang BQ, Li DC, Wang PG (2018) Prog Chem 30:831
11. Wexselblatt E, Gibson D (2012) J Inorg Biochem 117:220
12. Basu U, Banik B, Wen R, Pathak RK, Dhar S (2016) Dalton Trans 45:12992
13. Gabano E, Ravera M, Osella D (2014) Dalton Trans 43:9813
14. Liu H, Ma J, Li Y, Yue K, Li L, Xi Z, Zhang X, Liu J, Feng K, Ma Q, Liu S, Guo S, Wang PG, Wang C, Xie S (2019) J Med Chem 62:11324
15. Ma J, Liu H, Xi Z, Hou J, Li Y, Niu J, Liu T, Bi S, Wang X, Wang C, Wang J, Xie S, Wang PG (2018) Front Chem 6:386
16. Chen Z, Liang X, Zhang HY, Xie H, Liu JW, Xu YF, Zhu WP, Wang Y, Wang X, Tan SY, Kuang D, Qian XH (2010) J Med Chem 53:2589
17. Seliga R, Pilatova M, Sarissky M, Viglasky V, Walko M, Mojzis J (2013) Mol Biol Rep 40:4129
18. El-Azab AS, Alanazi AM, Abdel-Aziz NI, Al-Suwaidan IA, El-Sayed MAA, El-Sherbeny MA, Abdel-Aziz AAM (2013) Med Chem Res 22:2360
19. Chua EY, Davey GE, Chin CF, Dröge P, Ang WH, Davey CA (2015) Nucleic Acids Res 43:5285
20. Pérez JM, López-Solera I, Montero EI, Braña MF, Alonso C, Robinson SP, Navarro-Ranninger C (1999) J Med Chem 42:5482
21. Herrera JM, Mendes F, Gama S, Santos I, Navarro-Ranninger C, Cabrera S, Quiroga AG (2014) Inorg Chem 53:12627
22. Navas F, Mendes F, Santos I, Navarro RC, Cabrera S, Quiroga AG (2017) Inorg Chem 56:6175
23. Wang QP, Li GS, Liu ZF, Tan XX, Ding Z, Ma J, Li LJ, Li DC, Han J, Wang BQ (2018) Eur J Inorg Chem 40:4442
24. Wang QP, Tan XX, Liu ZF, Li GS, Zhang RY, Wei JJ, Wang SB, Li DC, Wang BQ, Han J (2018) Eur J Pharm Sci 124:127
25. Li GS, Zhang JF, Liu ZF, Wang QP, Chen Y, Liu M, Li DC, Han J, Wang BQ (2019) J Inorg Biochem 194:34
26. Wang QP, Chen Y, Li GS, Liu ZF, Ma J, Liu M, Li DC, Han J, Wang BQ (2019) Bioorg Med Chem 27:2112
27. Wang Q, Huang Z, Ma J, Lu X, Zhang L, Wang X, Wang PG (2016) Dalton Trans 45:10366
28. Ma J, Wang Q, Huang Z, Yang X, Nie Q, Hao W, Wang PG, Wang X (2017) J Med Chem 60:5736
29. Wang Q, Chen Y, Li G, Zhao Y, Liu Z, Zhang R, Liu M, Li D, Han J (2019) Bioorg Med Chem Lett 29:126670
30. Quaquebeke EV, Mahieu T, Dumont P, Dewelle J, Ribaucour F, Simon G, Sauvage S, Gaussin JF, Tuti J, Yazidi ME, Vynckt FV, Mijatovic T, Lefranc F, Darro F, Kiss R (2007) J Med Chem 50:4122
31. Göschl S, Schreiber-Brynzak E, Pichler V, Cseh K, Heffeter P, Jungwirth U, Jakupec MA, Bergerbcd W, Keppler BK (2017) Metallomics 9:309
32. Jungwirth U, Xanthos DN, Gojo J, Bytzek AK, Körner W, Heffeter P, Abramkin SA, Jakupec MA, Hartinger CG, Windberger U, Galanski M, Keppler BK, Berger W (2012) Mol Pharmacol 81:719
33. Wei Q, Dong JF, Zhao PR, Li MM, Cheng FL, Kong JM, Li LZ (2016) J Photochem Photobiol B 161:355
34. Zhao PR, Wei Q, Dong JF, Ding FF, Li JH, Li LZ (2016) J Coord Chem 69:2437
35. Li XL, Hu YJ, Wang H, Yu BQ, Yue HL (2012) Biomacromolecules 13:873
36. Yuan LX, Liu M, Liu GQ, Li DC, Wang ZP, Wang BQ, Han J, Zhang M (2017) Spectrochim Acta A 173:584
37. Yuan LX, Liu M, Sun B, Liu J, Wei XL, Wang ZP, Wang BQ, Han J (2017) J Mol Liq 248:330
38. Mayr J, Heffeter P, Groza D, Galvez L, Koellensperger G, Roller A, Alte B, Haider M, Berger W, Kowol CR, Keppler BK (2017) Chem Sci 8:2241
39. Yuan LX, Liu M, Shi YB, Yan H, Han J, Liu LY (2018) J Biomol Struct Dyn 37:2776